Potts models: Density of states and mass gap from Monte Carlo calculations

Nelson A. Alves, Bernd A. Berg, and Ramon Villanova
Supercomputer Computations Research Institute and Department of Physics, The Florida State University, Tallahassee, Florida 32306
(Received 14 June 1990; revised manuscript received 9 October 1990)

Monte Carlo simulations are performed for first-order phase-transition models. The three-dimensional three-state Potts model has a weak first-order transition. For this model we calculate the density of states on L^3 block lattices (L up to size 36) and obtain high-precision estimates for the leading partition-function zeros. The finite-size-scaling analysis of the first zero exhibits the expected convergence of the critical exponent ν toward $1/D$ for large L; in particular, we find $\nu=2.955(26)$ from our two largest lattices. Analysis of our specific-heat C_v data yields $l=0.080\,31(26)$ for the latent heat. Along another line of approach, we calculate the mass gap $m=1/\xi$ (ξ is the correlation length) for cylindrical L^2L_z lattices (L up to 24 and $L_z=256$). The finite size-scaling analysis of these results is also consistent with the convergence of ν toward $1/D$, but that the limiting value is $1/D$ is not yet conclusively established. Some theoretical arguments favor $\nu\to 0$ in case of a first-order transition in a cylindrical $L^{D-1}\infty$ geometry. Therefore, we also applied our approach to the 2D ten-state Potts model, which is known to have a strong first-order transition. In this case we find unambiguous evidence in favor of $1/D$ as the limiting value.

I. INTRODUCTION

The study of the character of a phase transition by means of numerical simulations has recently received considerable attention.[1-11] Particularly cumbersome is the precise determination of the critical parameters for models with temperature driven weak first-order phase transitions, and the distinction from a second-order phase transition may be hampered by circumstantial numerical evidence.[8,9] Finite-size effects play an important role and may lead to inconclusive infinite volume results. An example is the critical exponent ν resulting from our finite-size-scaling (FSS) analysis of the mass gap for the three-dimensional (3D) three-state Potts model and for the 4D SU(3) pure gauge theory, as we have initially reported in Refs. 3 and 12. In contrast to these models we obtained for second-order phase transition models, the 3D Ising model[13] and 4D SU(2) pure gauge theory,[3] ν estimates which are self-consistent and in good agreement with expectations from existing literature. Respectively, the 3D Ising and three-state Potts model are conjectured[14] to be in the same universality class as the 4D SU(2) and SU(3) lattice gauge theories. According to the renormalization-group fixed point picture a first-order phase transition for a L^D block geometry is characterized by a critical exponent[15] $\nu=1/D$, where D is the dimension of the system. Numerical Monte Carlo renormalization studies[16] have shown consistency with the expected $\nu=1/D$ value. However, for a cylindrical $L^{D-1}\infty$ geometry the situation is less clear. One finds the conjecture $\nu\to 0$ in the most detailed literature,[17] whereas earlier results from Ref. 18 support the limit value $1/D$ also in this geometry, in addition see Ref. 19.

In this paper we closely follow our previous work[13] to investigate the $L\to\infty$ limit value of ν by means of Monte Carlo (MC) simulations. The 3D three-state Potts model has a rather weak first-order transition.[6,7] Using histogram techniques[20,21,13] we explore the limit value of ν on L^3 block lattices, with L up to 36, and on cylindrical L^2L_z lattices, with L up to 24 and $L_z=256$. For the block geometry we find clear evidence for $\nu\to 1/D$ and, in addition, obtain a nonzero latent heat by FSS analysis of the specific heat. For the cylindrical geometry the results are also consistent with $\nu\to 1/D$, but the limiting value itself is not firmly established. In particular the data would not exclude an overshooting toward zero, the scenario favored by Ref. 17. To investigate this question further, we simulated a model with a strong first-order transition, namely, the 2D ten-state Potts model.[22,23] The cylindrical geometry is approximated by $L\times L_z$ lattices with L up to 24 and L_z up to 500. In this case we find convincing evidence for $\nu\to 1/D$, as is already indicated by the analytical results of Blöte and Nightingale[18] for much smaller sized systems.

The plan of our work is the following. In Sec. II we calculate the leading Lee-Yang[24] zeros of the partition function for the 3D three-state Potts model with high precision. Their FSS analysis leads us to estimates of the critical coupling β_c and the exponent ν. Further, we have calculated the specific heat C_v as a function of the coupling, the critical coupling defined as corresponding to the maximum of C_v, and by FSS analysis the latent heat of the transition. Due to some disagreement with the analysis of Ref. 7 we feel obliged to comment in an Appendix on the specific heat C_v for the 3D Ising model.

In Sec. III we develop our second approach using the correlation length. For the 2D ten-state and the 3D three-state Potts model we estimate β_c and the second value for ν. We also make use of previous analytical results[18] for 2D q-state Potts model and we obtain a scenario where the intensity of the transition plays an important role. The approach of $\nu\to 1/D$ (for $L\to\infty$) is found to be more pronounced the stronger the phase transition is. Section IV gives our outlook and conclusions.

II. MONTE CARLO CALCULATION OF THE PARTITION FUNCTION

We consider the 3D three-state Potts model in the L^3 block geometry. The Hamiltonian is given by

$$H=-\tfrac{3}{2}\sum_{\langle i,j\rangle}\delta_{\sigma_i\sigma_j}\ , \tag{2.1}$$

where the sum is over the nearest-neighbor spin pairs and $\sigma_i=0$, 1, or 2. The action changes in increments of 1.5, and for L even,

$$-4.5L^3\le H\le 0\ . \tag{2.2}$$

We have used the standard Metropolis algorithms and report MC calculations for the density of states for lattices of sizes $L=10$, 12, 14, 18, 22, 24, 30, and 36. All the MC runs had a cold start and for thermalization 50 000 sweeps were discarded before taking measurements. For $L=10$, 12, 14 we used 50×10^6 sweeps and 20×10^6 for the other lattices. The production sweeps were divided into 20 bins and the error analysis was made applying the jackknife method. For energy and spin expectation values we have checked that autocorrelation between subsequent bins vanish within the statistical noise.

A. Density of states

We have generated configurations $K=\{\sigma\}$ via a MC Markov chain with the Boltzmann weight

$$P(\{\sigma\})=e^{-\beta H(\{\sigma\})}\ .$$

To obtain the density of states we histogram the generated configurations with respect to the energy and obtain the partition function by reweighting. To give an example we depict in Fig. 1 the histogram for our largest lattice ($L=36$). For all lattices our simulations were done at $\beta_{\rm MC}=0.367\,06$. This value corresponds to the weighted average of the infinite volume critical temperature from Refs. 6 and 7. In case of the 3D Ising model we have further studied a patching procedure[13] to calculate the density of states by combining energy histograms from variant β values. For the leading zero (imaginary part) and the largest lattice the difference between results from three or more patches versus the result from a single histogram was about three times the statistical error bar of the individual results. Statistically, this is just indicative for a systematic error. However, for second-order phase transitions the calculation of partition-functions

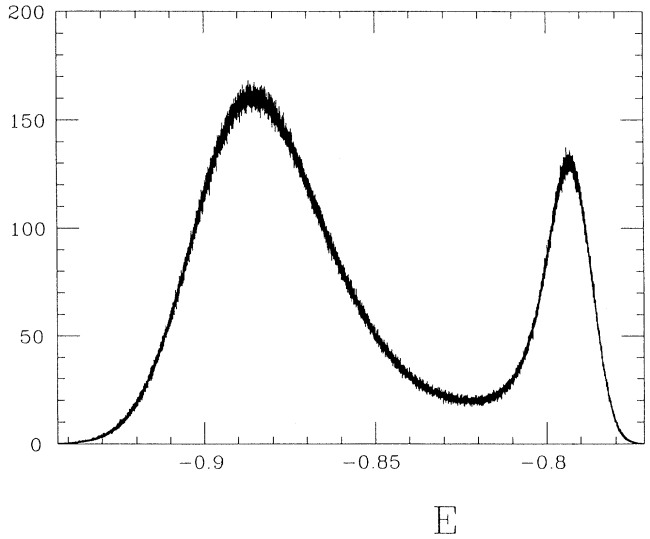

FIG. 1. 3D three-state Potts model energy per link histogram for $\beta=0.367\,06$ and $L=36$.

zeros is somewhat subtle. Single-energy histograms are almost normally distributed, but an exact Gaussian distribution does not have any zeros in the complex plane. The correct zeros rely on deviations from the Gaussian distribution and a good statistics on the tails of the central histogram is important (in MC simulations zeros due to statistical flukes are possible as well). In case of a double-peak structure this problem does not exist and one can anticipate that the tails lead only to statistically negligible corrections. Therefore, we have not carried out a further patching procedure in the present case. In the analog case of SU(3) lattice-gauge theory,[5] we have taken histograms at variant β values and can explicitly verify this stability of the leading partition-function zero for a first-order transition.

B. Partition-function zeros

Defining

$$u=\exp(-\tfrac{3}{2}\beta)\ , \tag{2.3}$$

the partition function becomes a polynomial of degree $3L^3+1$ in u. Its coefficients are determined by our numerically calculated spectral density. Using the Newton-Raphson method, as described in Ref. 25, we calculated the six zeros u_i^0 ($i=1,\ldots,6$) closest to the real axis. The results, in order of increasing imaginary part, are given in Tables I, II, and III.

TABLE I. First and second partition-function zeros for the 3D three-state Potts model.

L	$\mathrm{Re}(u_1^0)$	$\mathrm{Im}(u_1^0)$	$\mathrm{Re}(u_2^0)$	$\mathrm{Im}(u_2^0)$
10	0.576 265 2(59)	0.006 666 9(48)	0.573 526(17)	0.012 939(12)
12	0.576 471 7(49)	0.004 392 7(36)	0.574 653 2(90)	0.008 724 7(74)
14	0.576 594 0(37)	0.003 064 3(24)	0.575 335 1(69)	0.006 231 6(51)
18	0.576 678 2(64)	0.001 655 7(32)	0.576 000 7(60)	0.003 521 8(59)
22	0.576 700 7(60)	0.000 986 0(27)	0.576 309 5(57)	0.002 198 0(45)
24	0.576 706 1(39)	0.000 782 8(17)	0.576 403 9(34)	0.001 784 6(26)
30	0.576 693 1(28)	0.000 418 6(14)	0.576 541 2(25)	0.001 018 8(14)
36	0.576 674 0(34)	0.000 244 23(83)	0.576 592 0(30)	0.000 630 8(11)

TABLE II. Third and fourth partition-function zeros for the 3D three-state Potts model.

L	$\mathrm{Re}(u_3^0)$	$\mathrm{Im}(u_3^0)$	$\mathrm{Re}(u_4^0)$	$\mathrm{Im}(u_4^0)$
10	0.571 30(10)	0.017 81(14)	0.562 46(48)	0.018 35(37)
12	0.567 59(20)	0.011 95(16)	0.573 240(67)	0.012 191(65)
14	0.574 286(48)	0.008 882(44)	0.570 26(15)	0.008 94(17)
18	0.575 381(31)	0.005 128(39)	0.573 30(19)	0.005 69(14)
22	0.575 941(11)	0.003 204(16)	0.574 454(58)	0.003 494(70)
24	0.576 127 4(91)	0.002 629 8(82)	0.574 912(42)	0.002 837(32)
30	0.576 382 7(35)	0.001 535 6(25)	0.575 606(22)	0.001 912(33)
36	0.576 502 1(30)	0.000 968 9(23)	0.576 406 8(75)	0.001 273 3(72)

Let us define $u_c = u(\beta_c)$ and carry out the FSS analysis for the first zero. It is well known[26] that for sufficiently large L

$$u_1^0 - u_c = zL^{-1/\nu} , \tag{2.4}$$

where z is a complex constant in general. As for the 3D Ising model[13] we could rely on the relation

$$-\ln|u_1^0(L) - u_c| = \text{const} + \frac{1}{\nu}\ln(L) \tag{2.5}$$

to extract ν, using a MC estimate for the critical value β_c. However, for the present case it is more effective to use only the imaginary parts of the roots. The reason is not so much that the exact β_c is unknown, but that the L dependence of the real part is rather weak and consequently has a worse signal-to-noise ratio than the imaginary part. This makes Eq. (2.5) less favorable than the corresponding one with $u_1^0(L)$ replaced by $\mathrm{Im}u_1^0(L)$. However this two-parameter fit does not give acceptable values for the goodness of fit Q,[25] when extended over a range of three or more lattices. As discussed in Ref. 13 this indicates that our statistical noise is smaller than the finite-size corrections. Unfortunately, the four-parameter fit, successful for the 3D Ising model,[13] fails due to insufficiently accurate data in the present case. Therefore, the most pragmatic way to proceed is to rely on estimates from pairs of lattices,

$$y_T = \nu(L,L')^{-1} = \ln\left[\frac{\mathrm{Im}u_1^0(L')}{\mathrm{Im}u_1^0(L)}\right]\ln\left[\frac{L}{L'}\right]^{-1} . \tag{2.6}$$

Table IV shows the results obtained. For increasing $\min(L',L)$ the tendency $y_T \to D$ is obvious, although the needed systems are amazingly large. Our estimate closest to the infinite volume is $\nu^{-1} = 2.955(26)$ obtained by matching our largest lattices ($L = 30$ and 36).

C. Specific heat

Let us define the energy per link, its second moment, and the specific heat:

$$\langle E\rangle \equiv \frac{1}{DL^D}\langle H\rangle, \quad \langle E^2\rangle \equiv \left[\frac{1}{DL^D}\right]^2\langle H^2\rangle , \tag{2.7}$$

$$C_v(\beta) = \frac{\beta^2}{DL^D}(\langle H^2\rangle - \langle H\rangle^2) . \tag{2.8}$$

In a sufficiently small neighborhood of $\beta_{\mathrm{MC}} = 0.367\,06$ the β dependence can be obtained by reweighting. Figure 2 shows $C_v(\beta)$ for lattice sizes $L = 14$, 18, 22, 24, 30, and 36. For a first-order phase transition one has[23]

$$C_v|_{\max} = C_v(\beta_c^{C_v}) = A_1 + A_2 L^{A_3} , \tag{2.9}$$

with

$$A_3 = D \quad \text{and} \quad A_2 = \frac{(\beta_c)^2 D(E_+ - E_-)^2}{4} . \tag{2.10}$$

Here $+$ and $-$ refer to the high- and low-temperature phases, respectively. E_+ and E_- are peaks in the energy density corresponding to the maximum of the specific heat for $\beta = \beta_c^{C_v}$ [i.e., $\beta_c^{C_v}(L)$ is defined by Eq. (2.9)]. Introducing the latent heat $l = E_+ - E_-$, we have

$$l = \frac{2}{\beta_c}\left[\frac{A_2}{D}\right]^{1/2} . \tag{2.11}$$

Let us also define β_c^{zeros} from Eq. (2.3),

TABLE III. Fifth and sixth partition-function zeros for the 3D three-state Potts model.

L	$\mathrm{Re}(u_5^0)$	$\mathrm{Im}(u_5^0)$	$\mathrm{Re}(u_6^0)$	$\mathrm{Im}(u_6^0)$
10	0.570 77(40)	0.022 06(37)	0.566 8(21)	0.027 2(20)
12	0.572 40(23)	0.014 99(33)	0.572 73(42)	0.017 56(39)
14	0.573 36(23)	0.010 83(19)	0.573 82(31)	0.012 66(29)
18	0.574 73(22)	0.006 15(20)	0.575 13(20)	0.007 33(17)
22	0.575 726(37)	0.004 025(39)	0.575 753(65)	0.004 915(57)
24	0.575 978(23)	0.003 403(32)	0.575 787(87)	0.004 141(83)
30	0.576 270(14)	0.001 998(12)	0.576 223(28)	0.002 468(32)
36	0.575 912(25)	0.001 359(22)	0.576 353(21)	0.001 535(16)

TABLE IV. Table of $v(L,L')^{-1}$ for the 3D three-state Potts model, obtained by Eq. (2.6).

L'	$L=14$	$L=18$	$L=22$	$L=24$	$L=30$	$L=36$
10	2.3103(32)	2.3698(35)	2.4240(36)	2.4467(26)	2.5195(31)	2.5816(27)
12	2.3362(74)	2.4064(52)	2.4649(47)	2.4884(34)	2.5655(38)	2.6302(32)
14		2.4495(83)	2.5088(63)	2.5319(43)	2.6119(45)	2.6782(37)
18			2.583(17)	2.604(10)	2.6919(76)	2.7611(56)
22				2.652(40)	2.762(14)	2.8337(89)
24					2.805(18)	2.873(10)
30						2.955(26)

$$\beta_c^{\text{zeros}}(L)=-\tfrac{1}{3}\ln\{[\mathrm{Re}u_1^0(l)]^2+[\mathrm{Im}u_1^0(L)]^2\}\ . \quad (2.12)$$

It is interesting to compare both effective critical β's. This is done in Table V where also $C_v|_{\max}$ values are given. Table VI gives $\beta_c^{C_v}$, $C_v|_{\max}$ data from Refs. [6 and 7]. Following Ref. 23 the infinite volume critical β_c is calculated from

$$T_c^{C_v}(L)=T_c+AL^{-D} \text{ or } \beta_c^{C_v}(L)=\beta_c+BL^{-D}\ . \quad (2.13)$$

The results from least-square fits of our data combined with Ref. 7 data are given in Table VII. The infinite volume critical β,

$$\beta_c=0.367\,015\,4\pm0.000\,006\,4 \quad (2.14)$$

may be considered as the most convincing estimate from this table and is used in the latent heat fits.

Table VIII shows results obtained for A_1, A_2, A_3, and l from the fits of Eq. (2.9) using our data. Figure 3 shows the behavior of $C_v|_{\max}L^{-3}$ for $A_3=3$. This fit has $Q=0.59$ and gives

$$A_1=3.661(64) \text{ and } A_2=0.000\,651\,6(42)\ ,$$

i.e., (2.15)

$$l=0.080\,31(26)\ .$$

The latent heat result reported in Ref. 6 is $l=0.080(4)$.

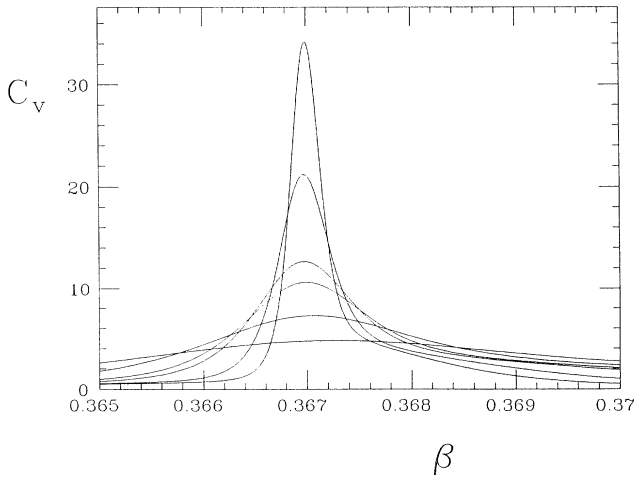

FIG. 2. 3D three-state Potts model specific heat for $L=14$, 18, 22, 24, 30 and 36.

Table IX shows the parameters A_1, A_2, A_3, and the latent heat when using data from Ref. 7. Table X combines $L=30$, 36 from our data and $L=30$, 36, 42, 48 from Ref. 7. Overall there is satisfactory agreement. For an analysis of the 3D Ising model specific heat data see the Appendix.

Exponential corrections to the scaling law (2.9) were analyzed in Refs. 21 and 27. This leads to the four-parameter fit:

$$C_v|_{\max}=A_1+A_2L^3+A_4\exp\left[-\frac{L}{A_5}\right]\ . \quad (2.16)$$

For the cases of Table VIII we found this fit unstable (using the program MRQMIN from Ref. 25). Including now also the smaller lattices $L=10$, 12, and 14 yields a stable fit for the range $L=10$–36: $A_1=4.57(22)$, $A_2=0.000\,631\,4(60)$, $A_4=-5.974(62)$, $A_5=10.2(1.0)$, but with $Q=0.02$ the goodness of fit is barely acceptable anymore.

III. CORRELATION LENGTH CALCULATION

Following our previous approach,[13] we have used the MC transfer matrix method on a cylindrical $L^{D-1}L_z(D=2,3)$ geometry with periodic boundary conditions. For the 2D ten-state Potts model our lattice size L goes up to 24 with $L_z=256$ for $L\le16$, for $L=24$ we

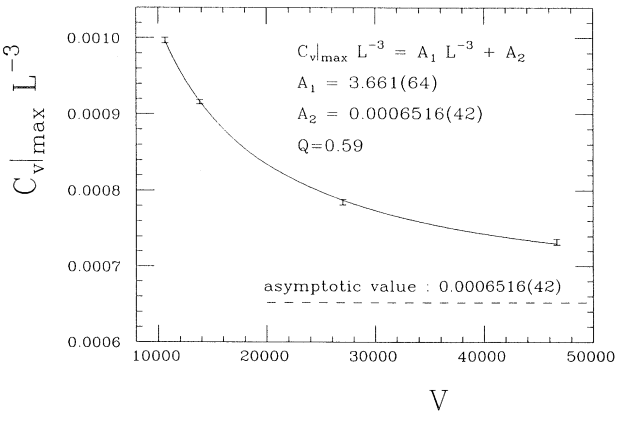

FIG. 3. 3D three-state Potts model volume dependence of the specific heat.

TABLE V. Comparison for effective critical β's: β_c^{zeros} and $\beta_c^{C_v}$; also the maximum of the specific heat.

L	β_c^{zeros}	$\beta_c^{C_v}$	$C_v\|_{\max}$
10	0.367 413 6(68)	0.367 910 9(64)	2.9605(25)
12	0.367 200 0(57)	0.367 486 2(52)	3.8165(39)
14	0.367 068 5(43)	0.367 245 5(39)	4.7886(46)
18	0.366 977 8(74)	0.367 053 1(71)	7.263(19)
22	0.366 953 6(69)	0.366 989 1(66)	10.615(39)
24	0.366 947 7(45)	0.366 972 7(43)	12.659(38)
30	0.366 963 2(32)	0.366 972 6(31)	21.19(10)
36	0.366 985 4(39)	0.366 989 3(39)	34.18(18)

have increased L_z to 500 and the same for all L at $\beta=1.426\,06$, which is close to the known critical coupling[22]

$$\beta_c=\ln(1+\sqrt{q})=1.426\,062\,4\ldots . \tag{3.1}$$

For the 3D three-state Potts model we have also used L up to 24 with fixed $L_z=256$ for $L\le 16$. But for $L=24$ we had to decrease L_z to 222 to avoid technical problems with our vector length. The long direction L_z was maintained as long as possible to approximate ∞ for achieving accurate and reliable correlation length estimates.

The zero-momentum correlation function,[13]

$$C(z)=\langle S_0 S_z\rangle \sim \left[\frac{\lambda_1}{\lambda_0}\right]^z+\left[\frac{\lambda_1}{\lambda_0}\right]^{L_z-z} \quad (\text{for } z\to\infty), \tag{3.2}$$

where λ_0 is the largest and λ_1 the next-largest eigenvalue of the transfer matrix, allows numerical calculation of the correlation length

$$\xi=m^{-1}=\ln\left[\frac{\lambda_0}{\lambda_1}\right] \tag{3.3}$$

by means of calculating effective masses $m(z)$ at distance z in the long direction. The MC estimator $C_{\text{MC}}(z)$ for $C(z)$ is obtained measuring $S_{z_1}S_{z_2}$ at distance $d(z_1,z_2)=z$ and our effective masses are defined by the fit

$$\frac{C_{\text{MC}}(z)}{C_{\text{MC}}(z-1)}=\frac{\exp[-m(z)z]+\exp[-m(z)(L_z-z)]}{\exp[-m(z)(z-1)]+\exp[-m(z)(L_z-z+1)]} . \tag{3.4}$$

We elect our effective mass $m(z_0)$, chosen at an appropriate distance z_0, as corresponding to the asymptotic value $m=m(\infty)$. This issue was considered in detail in Ref. 13. Our Potts model results are given in Tables XI and XII.

The critical exponent ν is obtained using FSS in a neighborhood of the critical point.[17,18,28,29] Let $P(\beta)$ be a physical observable with the critical behavior

$$P(\beta)\sim(\beta-\beta_c)^{-\rho} , \tag{3.5}$$

where ρ is the critical exponent of P. Using FSS one obtains

$$P(\beta_c,L)\sim L^{\rho/\nu} . \tag{3.6}$$

For our study we need the special cases

$$m(\beta_c,L)=\frac{c}{L}+O\left[\frac{1}{L^2}\right]$$

TABLE VI. Critical couplings and maximum of the specific heat. For the definition of β_c^{fit} see Eq. (2.10) of Ref. 6, first paper.

	Reference 6	Reference 7	
L	β_c^{fit}	$\beta_c^{C_v}$	$C_v\|_{\max}$
22		0.367 025(28)	10.98(17)
24	0.366 70(1)	0.366 990 0(81)	12.856(69)
26		0.366 985(23)	15.22(26)
30	0.366 91(1)	0.366 965 7(94)	20.98(22)
36	0.366 99(1)	0.366 991 3(81)	34.29(33)
42		0.366 992 7(81)	52.45(67)
48	0.367 025(25)	0.367 011 5(81)	78.4(1.0)
∞	0.367 08(2)	0.367 026(27)	

TABLE VII. $L=22,24,30,36$ correspond to our data. $L=22,24,26,30,36,42,48$ to data from Ref. 7.

L	$\beta_c(\infty)$	Q
22–48	0.366 987 5(35)	2.1E-5
24–48	0.366 992 9(39)	6.5E-4
26–48	0.367 013 2(62)	0.51
30–48	0.367 015 4(64)	0.74
36–48	0.367 019(12)	0.52

and (3.7)

$$\left.\frac{d}{d\beta}m(\beta,L)\right|_{\beta=\beta_c} \sim L^{-1-1/\nu}$$

to estimate the infinite volume critical coupling β_c and the critical exponent ν. The subsequent two sections analyze our numerical $m(\beta,L)$ results. For the presentation we deviate from the chronological order of our investigation and begin with the 2D model.

A. 2D ten-state Potts model

The 2D ten-state ($q=10$) Potts model is defined by the Hamiltonian

$$H=-\sum_{\langle i,j\rangle}\delta_{\sigma_i\sigma_j},\quad \sigma_i=1,2,\ldots,10\ . \tag{3.8}$$

The q-spin states on each lattice site can be represented by a set of q unit vectors pointing in q symmetric directions in a $(q-1)$-dimensional space,[30] which is the appropriate formalism to calculate zero-momentum correlation functions.

Our results were obtained with 2^{19} sweeps and measurements, with an additional of 16 000 sweeps for reaching thermalization at the beginning of each (β,L) data point. We have used 2^6 bins to estimate error bars in our Table XI. In Fig. 4 we plot $Lm(\beta,L)$ versus β. For finite L we define crossover points $\beta_0(L,L')$ of two lattices L,L', with $L>L'$, as finite-volume estimates of β_c. The infinite volume critical point β_c is obtained as

$$\lim_{L'\to\infty}\beta_0(L,L')=\beta_c\ . \tag{3.9}$$

The straight lines in Fig. 4 are least-square fits to our $Lm(\beta,L)$ data. To optimize the accuracy of the fitted lines we use β values as far apart from one another as possible, while keeping the goodness of fit Q at acceptable values. This, on the other hand, determines an admissable range of β points for each L. Table XI contains our complete data set. In Fig. 4 we have restricted our straight lines to the actually used points.

The fixed points $\beta_0(L,L')$ are given in the upper triangle of Table XIII. The values in this table show a convergence toward the theoretical value

$$\beta_c=1.426\,062,\ldots\ . \tag{3.10}$$

Neglecting finite-size systematic errors our best estimate

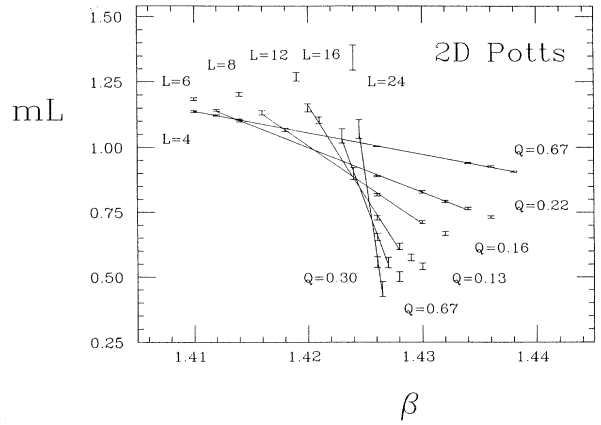

FIG. 4. 2D ten-state Potts model mass gap data.

is

$$\beta_c\sim\beta_0(24,16)=1.4256\pm0.0001\ . \tag{3.11}$$

We determine the critical exponent ν by using Eq. (3.7). The derivatives around the fixed points are promptly obtained from the straight lines in Fig. 4, and Table XI contains our estimates for $(d/d\beta)Lm(\beta,L)|_{\beta=\beta_c}$. In Fig. 5 we plot the L dependence of these derivatives in a log-log scale. The linear regression according to Eq. (3.7) gives us an estimate for the critical exponent ν. Two linear fits, from $L_{\min}=4$ to $L_{\max}=24$ and from $L_{\min}=6$ to $L_{\max}=24$, are depicted in this figure. The first least-square fit gives us an unacceptable Q value ($\sim10^{-3}$) while the second one, with $Q=0.32$, means we have a confident fit to extract the ν value

$$\nu=0.493\pm0.008\ . \tag{3.12}$$

Now we explore the ν dependence of L using this two point fit approach and relying on the exact results for $(d/d\beta)Lm(\beta,L)$ from the transfer matrix method.[18] Results for 2D q-state Potts model with $q=8$ and $q=64$ are

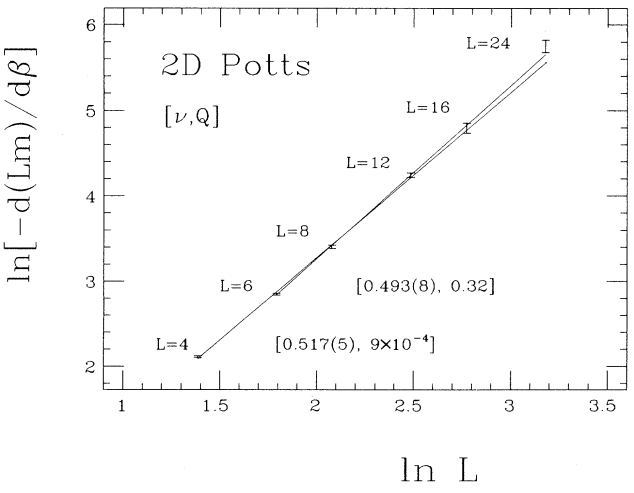

FIG. 5. 2D ten-state Potts model ν fits.

TABLE VIII. Different fits for Eq. (2.9), with its respective latent heat using our data. [For β_c we use $\beta_c = 0.367\,015\,4(64)$ obtained in Table VII.]

L	A_1	A_2	A_3	Q	l
18–36	3.101(99)	0.000 98(11)	2.890(32)	0.033	
18–36	3.420(29)	0.000 664 5(29)	3	2.8E-4	
22–36	4.00(34)	0.000 49(14)	3.080(80)	0.80	
22–36	3.661(64)	0.000 651 6(42)	3	0.59	0.080 31(26)
24–36	4.12(57)	0.000 45(20)	3.10(12)		
24–36	3.626(87)	0.000 653 0(48)	3	0.40	0.080 40(30)
30–36	3.35(34)	0.000 661(11)	3		0.080 89(67)

TABLE IX. Data from Ref. 7. To be compared with Table VIII.

L	A_1	A_2	A_3	Q	l
30–48	3.7(1.8)	0.000 45(30)	3.11(17)	0.44	
30–48	2.61(40)	0.000 679 4(94)	3	0.61	0.082 01(57)

TABLE X. $L = 30, 36$ of our data combined with $L = 30, 36, 42, 48$ data from Ref. 7. This table should be compared with Tables VIII and IX.

L	A_1	A_2	A_3	Q	l
30–48	4.4(1.0)	0.000 37(16)	3.15(11)	0.75	
30–48	3.03(24)	0.000 670 4(68)	3	0.56	0.081 46(41)
36–48	2.28(69)	0.000 684(14)	3	0.64	0.082 28(84)

TABLE XI. Mass gap estimates: $Lm(\beta, L)$ is given for 2D Potts model. By $[z]$ we denote the distance at which the effective mass is taken to be asymptotic. Data marked by an asterisk are not used for the straight-line fits, because they lead to unacceptable Q's. The estimated derivatives as obtained from Fig. 4 are shown for all L's.

β	$L=4$	$L=6$	$L=8$	$L=12$	$L=16$	$L=24$
1.410 00	1.1368(28)[4]	1.1846(50)*[4]				
1.412 00	1.1223(25)[4]	1.1415(39)[4]				
1.414 00	1.1065(24)[4]	1.1005(43)[4]	1.2032(75)*[5]			
1.416 00			1.1323(79)[5]			
1.418 00			1.0668(64)[5]	1.342(14)*[5]		
1.419 00				1.270(16)*[5]		
1.420 00				1.151(15)[5]		
1.421 00				1.104(12)[5]		
1.423 00					1.043(27)[6]	
1.424 00					0.899(24)[6]	1.343(49)*[6]
1.424 50						1.069(36)[6]
1.426 06	1.0039(16)[4]	0.8900(33)[4]	0.8174(48)[5]	0.7288(86)[5]	0.654(15)[6]	0.557(20)[6]
1.426 50						0.454(29)[6]
1.426 60						0.456(19)*[6]
1.427 00					0.556(20)[6]	
1.428 00				0.618(13)[5]	0.501(19)*[6]	
1.429 00				0.575(13)*[5]		
1.430 00		0.8287(49)[5]	0.7120(57)[5]	0.540(13)*[5]		
1.432 00		0.7913(46)[5]	0.6682(73)*[5]			
1.434 00	0.9398(25)[4]	0.7646(48)[5]				
1.436 00	0.9268(27)[4]	0.7324(48)*[5]	0.5936(73)*[5]			
1.438 00	0.9070(24)[4]	0.7155(41)*[5]				
$\frac{d}{d\beta} Lm(\beta, L)\|_{\beta=\beta_c}$	−8.237(86)	−17.25(20)	−30.13(56)	−69.7(1.9)	−120.8(7.2)	−314(23)

shown in Fig. 6. The L behavior for ν [defined as $\nu=\nu(L_{\min},L_{\max})$, where $L_{\min}$ and $L_{\max}$ are as before the limits for our linear regression and $L_{\max}$ is always the largest available lattice size] is given for $q=8$, 64. The convergence toward $1/D$ is quickly achieved for $q=64$. For $q=8$ (a weaker phase transition than $q=64$) no conclusive infinite volume limit is obtained from these small lattice sizes ($L_{\max}=8$). For $q=10$ (an only slightly stronger phase transition than $q=8$) our MC transfer matrix method allows larger lattices and then convergence toward $1/D$ becomes rather convincing from $L_{\min}\geq 6$ on. In conclusion, it seems that for temperature driven first-order phase transitions some theoretical work remains to be done on the interesting subject of geometry dependent FSS theory.[17]

B. 3D three-state Potts model

For the 3D three-state Potts model our statistics per data point (β,L) relies on 320 000 MC sweeps, with measurements every 10 sweeps. An additional 8000 sweeps were always discarded for thermalization. We have used 20 bins to estimate error bars. Our $Lm(\beta,L)$ estimates are given in Table XII. Following our previous procedure results for $Lm(\beta,L)$ are presented in Fig. 7, where some points are not included because of their unacceptable Q values. Table XIII also contains our fixed points for the 3D three-state Potts model. Our best estimate is

$$\beta_c\sim\beta_0(24,16)=0.366\,91\pm0.000\,02\ . \tag{3.13}$$

Of course, its accuracy cannot compete with Eq. (2.14), but clearly both sets of results are consistent.

The ν estimates for this model are shown in Fig. 8. The linear regression for ν still has unacceptable Q values. However, the large L behavior for ν defined as $\nu=\nu(L_{\min},L_{\max})$ shows a clear trend toward $1/D$. Bearing in mind the results of the previous section, the rather weak first-order transition is conjectured to be responsible for the slow convergence. Within its statistical errors

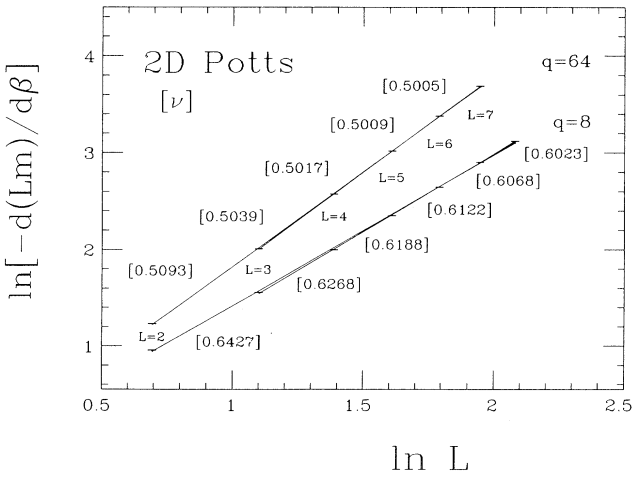

FIG. 6. 2D q-state Potts model ($q=8,64$) ν fits from exact results (Ref. 18).

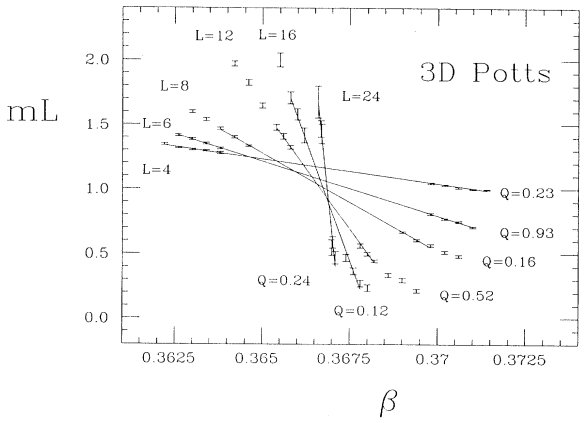

FIG. 7. 3D three-state Potts model mass gap data.

the estimate from $L_{\min}=16$, $L_{\max}=24$ is just $1/D$, but with the presented trend from other lattices one does not feel confident to exclude accidental agreement. The relative error of this estimate is about 5%, whereas it is less than 1% for the final estimate from the partition-function zeros.

IV. SUMMARY AND CONCLUSIONS

We studied models with a first-order phase transition and different methods were used to extract the critical exponent ν. In the cylindrical geometry rapid convergence toward the infinite volume limit is found in two rather extreme cases, namely, for the 3D Ising model[13] and its second-order transition and, as presented here, for the strong first-order transition of the 2D ten-state Potts model, even more pronounced for the 2D 64-state Potts model.[18] In contrast the convergence is found to be modest for the 3D three-state Potts model and its weak first-order transition.

Altogether, if one is mainly interested in critical ex-

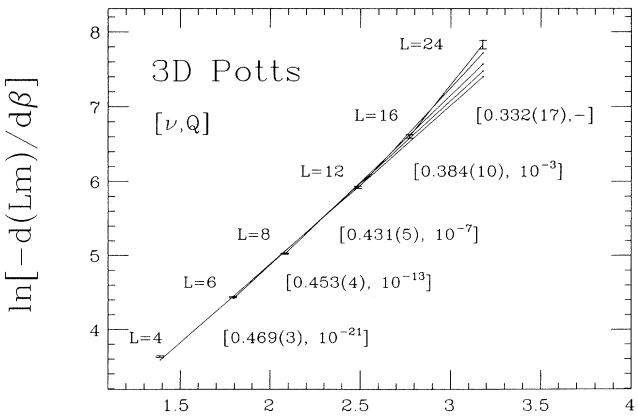

FIG. 8. 3D three-state Potts model ν fits.

TABLE XII. Mass gap estimates: $Lm(\beta,L)$ is given for 3D Potts model, otherwise as Table XI. The estimated derivatives as obtained from Fig. 7 are shown for all L's.

β	$L=4$	$L=6$	$L=8$	$L=12$	$L=16$	$L=24$
0.362 20	1.3445(68)[4]					
0.362 60	1.3177(51)[4]	1.4146(80)[4]				
0.363 00	1.3035(64)[4]	1.3859(78)[4]	1.600(10)*[5]			
0.363 40	1.2944(59)[4]	1.3517(71)[4]	1.538(12)*[5]			
0.363 80	1.2788(80)[4]	1.3136(65)[4]	1.4693(96)[5]	1.971(20)*[7]		
0.364 20			1.4022(95)[5]	1.823(22)*[7]		
0.364 60			1.3315(60)[5]			
0.365 00				1.647(20)*[7]		
0.365 40				1.478(23)[7]		
0.365 50					1.999(54)*[8]	
0.365 60				1.408(22)[7]		
0.365 80				1.322(14)[7]	1.708(45)[8]	
0.366 00					1.580(44)[8]	
0.366 20					1.417(58)[8]	
0.366 60						1.676(123)[9]
0.366 68						1.467(63)[9]
0.366 70						1.428(77)[9]
0.367 00						0.547(59)[9]
0.367 02						0.588(43)[9]
0.367 10						0.469(48)[9]
0.367 40					0.468(28)[8]	
0.367 60					0.365(25)[8]	
0.367 80				0.560(16)[7]	0.272(26)[8]	
0.368 00				0.498(14)[7]	0.235(26)*[8]	
0.368 20				0.443(11)[7]		
0.368 60				0.335(16)*[7]		
0.369 00			0.6653(57)[5]	0.297(17)*[7]		
0.369 40			0.6029(78)[5]	0.216(15)*[7]		
0.369 80	1.0460(67)[4]	0.8074(69)[4]	0.5649(94)[5]			
0.370 20	1.0319(44)[4]	0.7709(63)[4]	0.512(10)*[5]			
0.370 60	1.0126(62)[4]	0.7471(61)[4]	0.4819(96)*[5]			
0.371 00	0.9999(45)[4]	0.7062(53)[4]				
0.371 40	0.9970(34)[4]					
$\frac{d}{d\beta}Lm(\beta,L)\|_{\beta=\beta_c}$	−37.70(44)	−84.49(65)	−151.9(1.2)	−372.5(5.4)	−739(19)	−2507(141)

ponents and latent heat for (possibly weak) first-order transitions, the L^D block geometry seems to be more suitable for a MC investigation than the $L^{D-1}\infty$ cylindrical geometry. For SU(3) gauge theory[5] as well as for all Potts model cases (results for the 2D ten-state Potts model are reported elsewhere[31]) the FSS analysis of the partition-function zeros yields the exponent ν in a rather efficient way. Naturally, for simulations large L values are important and easier reached in the block than in the cylindrical geometry. In principle this advantage may be offset by an expected faster convergence in the cylindrical case, but in practice this does not really seem to happen for the first-order transitions. In addition, the FSS analysis of the specific heat from L^D lattices gives a self-consistent (means acceptable Q) determination of a nonzero latent heat for each of the first-order models. This seems to be the most direct and convincing way to establish that a transition is of first order.

TABLE XIII. MC estimates of $\beta_c(L,L')$. From up to down, the first "triangle" corresponds to 2D ten-states Potts model data set and the second one to 3D Potts model.

L'	$L=4$	$L=6$	$L=8$	$L=12$	$L=16$	$L=24$
4		1.4138(4)	1.4178(3)	1.4217(2)	1.4230(2)	1.4246(2)
6	0.364 64(8)		1.4206(3)	1.4231(2)	1.4238(2)	1.4250(1)
8	0.365 40(4)	0.365 92(7)		1.4239(2)	1.4242(2)	1.4252(1)
12	0.366 17(3)	0.366 42(3)	0.366 57(4)		1.4245(3)	1.4254(1)
16	0.366 52(3)	0.366 65(3)	0.366 73(3)	0.366 84(5)		1.4256(1)
24	0.366 80(2)	0.366 84(2)	0.366 86(2)	0.366 90(2)	0.366 91(2)	

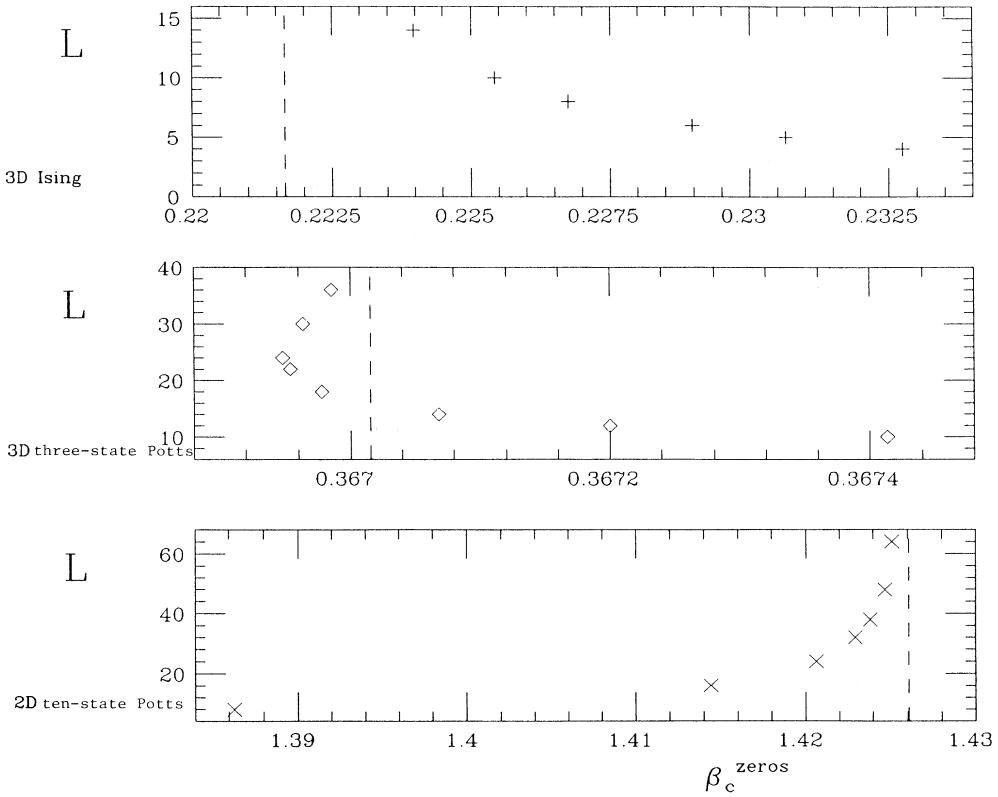

FIG. 9. $\beta_c^{zeros}(L)$ for 3D Ising, 3D three-state Potts, and 2D ten-state (Ref. 31) Potts models.

Finally, an observation, graphically presented in Fig. 9, may be worthwhile to notice. For the 3D Ising model (second-order phase transition) the effective critical β_c^{zeros} approach $\beta_c(\infty)$ from above, $[\beta_c^{zeros} > \beta_c(\infty)]$. For the 2D ten-state Potts model (strong first-order phase transition) the approach to $\beta_c(\infty)$ is from below $[\beta_c^{zeros}(L) < \beta_c(\infty)]$. Curiously, for the 3D three-state Potts model we have a second-order-like behavior for $L \leq 22$ and a first order as for $L \geq 24$. The model does not seem to "choose" its order until $L \simeq 24$.

One may use α/ν as a measure for the strength of a second-order transition. In this sense the 3D Ising model $\alpha/\nu \sim 0.11$ (see the Appendix) has a weak second-order transition. First-order transitions have $\alpha/\nu = D$ and the latent heat provides a measure for their strength. It may be interesting to find and to investigate a model with a strong second-order phase transition, i.e., with α/ν only slightly smaller than D. Similar to first-order transitions, we would expect the block geometry to be more appropriate for such a study. On the other hand, for a weak second-order transition [at least we have some evidence in case of 4D SU(2) lattice gauge theory] it may well be possible that the MC transfer matrix approach on cylindrical lattices yields a more efficient determination of ν than the FSS analysis of zeros. Presently, the issue is not yet completely clarified, some work is in preparation.[32]

ACKNOWLEDGMENTS

We thank R. V. Gavai, F. Karsch, B. Petersson, and A. Hasenfratz for providing valuable help with computer programs, and J. Vinals for useful comments. The Monte Carlo data were produced on the ETA10-*G* at the Florida State University. This work was partially funded by the Department of Energy under Contracts DE-FC05-85ER2500 and DE-FG05-87ER40319. N. Alves was supported by Conselho Nacional de Desenvolvimento Científico e Tecnológico (CNPq) Brazil, and by the Alexander von Humboldt Foundation in Germany.

APPENDIX

We would like to comment on the results $\alpha/\nu = 0.30(3)$ for the 3D Ising model claimed in Ref. 7 from the fit

$$C_v|_{\max} = A_1 L^{\alpha/\nu} , \tag{A1}$$

as their data was not precise enough to get the subleading term. We carried out FSS fits of the form[33]

$$C_v(\beta_c = 0.221\,650) = A_1 L^{\alpha/\nu} + A_3 . \tag{A2}$$

Using our $L = 14$ lattice[13] and combining it with data given in Ref. 34, we obtain

$$\alpha/\nu = 0.127 \pm 0.020 , \tag{A3}$$

with a goodness of fit $Q = 0.93$. In contrast to $\alpha/\nu = 0.30(3)$ this result is now consistent with the hyperscaling relation $D\nu = 2 - \alpha$, the analytical estimates[35] $\alpha = 0.110(5)$, $\nu = 0.630(2)$, and a recent numerical FSS analysis[36] (along different lines as presented here).

[1]P. Bacilieri *et al.,* Phys. Rev. Lett. **61**, 1545 (1988); Phys. Lett. B **224**, 333 (1989).
[2]F. Brown *et al.,* Phys. Rev. Lett. **61**, 2058 (1988).
[3]B. A. Berg, R. Villanova, and C. Vohwinkel, Phys. Rev. Lett. **62**, 2433 (1989).
[4]M. Fukugita, M. Okawa, and A. Okawa, Nucl. Phys. **B337**, 181 (1990).
[5]N. A. Alves, B. A. Berg, and S. Sanielevici, Phys. Rev. Lett. **64**, 3107 (1990).
[6]R. V. Gavai, F. Karsch, and B. Petersson, Nucl. Phys. **B322**, 738 (1989); S. Gupta, A. Irbäk, B. Petersson, R. V. Gavai, and F. Karsch, *ibid.* **B329**, 263 (1990).
[7]M. Fukugita, H. Mino, M. Okawa, and A. Ukawa, J. Stat. Phys. **59**, 1397 (1990).
[8]J. F. McCarthy, Phys. Rev. B **41**, 9530 (1990).
[9]P. Peczak and D. P. Landau, Phys. Rev. B **39**, 11 932 (1989).
[10]A. Billoire, R. Lacaze, and A. Morel, Nucl. Phys. B (Proc. Suppl.) **17**, 230 (1990).
[11]M. Fukugita, H. Mino, M. Okawa, and A. Ukawa, J. Phys. A **23**, L561 (1990).
[12]B. A. Berg and N. A. Alves, Nucl. Phys. B (Proc. Suppl.) **17**, 194 (1990).
[13]N. A. Alves, B. A. Berg, and R. Villanova, Phys. Rev. B **41**, 383 (1990).
[14]B. Svetitsky and G. Yaffe, Phys. Rev. B **21**, 3976 (1980).
[15]M. E. Fisher and A. N. Berker, Phys. Rev. B **26**, 2507 (1982).
[16]K. Decker, A. Hasenfratz, and P. Hasenfratz, Nucl. Phys. **B295** [FS21], 21 (1988).
[17]V. Privman and M. E. Fisher, J. Stat. Phys. **33**, 385 (1983). (For the conjecture $\nu \rightarrow 0$ see p. 411.)
[18]H. W. Blöte and M. P. Nightingale, Physica **112A**, 405 (1982).
[19]E. Brezin and J. Zinn-Justin, Nucl. Phys. **B257** [FS14], 867 (1985).
[20]R. McDonald and K. Singer, Discuss. Faraday Soc. **43**, 40 (1967); M. Falcioni, E. Marinari, M. L. Paciello, G. Parisi, and B. Taglienti, Phys. Lett. **108B**, 331 (1982); E. Marinari, Nucl. Phys. **B235** [FS11], 1233 (1984).
[21]A. M. Ferrenberg and R. H. Swendsen, Phys. Rev. Lett. **61**, 2635 (1988).
[22]F. Y. Wu, Rev. Mod. Phys. **54**, 235 (1982).
[23]M. S. Challa, D. P. Landau, and K. Binder, Phys. Rev. B **34**, 1841 (1986).
[24]C. N. Yang and T. D. Lee, Phys. Rev. **87**, 404 (1952); **87**, 410 (1952).
[25]W. Press *et al., Numerical Recipes* (Cambridge University Press, London, 1988).
[26]C. Itzykson, R. B. Pearson, and J. B. Zuber, Nucl. Phys. **B220** [FS8], 415 (1983).
[27]O. de Alcantara Bonfim (unpublished).
[28]M. E. Fisher, in *Critical Phenomena,* proceedings of the 51st Enrico Fermi Summer School, Varena, edited by M. S. Green (Academic, New York, 1972).
[29]E. Brezin, J. Phys. (Paris) **43**, 15 (1982) and references given therein.
[30]R. K. P. Zia and D. J. Wallace, J. Phys. A Math. Gen. **8**, 1495 (1975).
[31]B. A. Berg, A. Hasenfratz, and R. Villanova (unpublished).
[32]N. A. Alves, B. A. Berg, and S. Sanielevici (unpublished).
[33]M. N. Barber, R. B. Pearson, D. Toussaint, and J. L. Richardson, Phys. Rev. B **32**, 1720 (1985).
[34]G. Bhanot, D. Duke, and R. Salvador, Phys. Rev. B **33**, 7841 (1986).
[35]M. E. Fisher and J. H. Chen, J. Phys. (Paris) **46**, 1645 (1985); A. J. Liu and M. E. Fisher, Physica **A156**, 35 (1989).
[36]Pik-Yin Lai and K. K. Mon, Phys. Rev. Lett. **62**, 2608 (1989).